Synthesis, Characterization, and Electronic and Optical Properties of Donor−Acceptor Conjugated Polymers Based on Alternating Bis(3-alkylthiophene) and Pyridine Moieties

Hong-Fang Lu, Hardy S. O. Chan, and Siu-Choon Ng*

Department of Chemistry, National University of Singapore, Singapore 119260, Singapore

Received July 11, 2002; Revised Manuscript Received October 21, 2002

ABSTRACT: A novel series of conjugated polymers comprising alternating π-excessive bis(3-alkylthiophene) and π-deficient 2,5-pyridine (or 2,6- or 3,5-pyridine) moieties were synthesized using a Stille coupling approach and characterized by FT-IR, NMR, UV−vis, fluorescence spectroscopy, gel permeation chromatography (GPC), thermogravimetric analysis (TGA), electrochemical analysis, and X-ray photoelectron spectroscopy (XPS). The derived polymers were highly soluble in common organic solvents and trifloroacetic acid. The electronic and optical properties of these polymers were closely related to the polymer backbone structures. Polymers containing 2,6-/3,5-pyridine moieties exhibited blue shifts in UV and fluorescent spectra relative to those containing 2,5-pyridine analogues, and polymers containing 3,5-pyridine units depicted the highest thermal stability, UV absorption energy, fluorescence energy, and reduction potentials. The electrochemical behavior of these new polymers showed facile n-doping and p-doping properties. The lower reduction potential of these polymers implied their good electron-transporting and easy electron-injection properties due to the presence of the electron-withdrawing pyridine unit. The optical properties of the polymers in trifloroacetic acid were also investigated. XPS studies performed on both neutral and doped states implied the formation of charge carriers in the polymer backbones when doped.

Introduction

In recent years, many donor−acceptor conjugated polymers have been studied showing unique optoelectronic properties with potential applicability in devices. Thus, CN−PPVs in which poly(phenylvinylene)s were functionalized with flexible alkyl/alkoxy and CN side chains depicted high electron affinities and electron-transporting properties, depicting interesting properties in optical absorption,[1] electronic structure,[2] photoinduced absorption, excitation spectra,[3] luminescence efficiency,[4] characteristics of LEDs,[5−7] and photodiodes.[8] The presence of donor and acceptor functionalities in the polythienylene backbone has been reported to result in the formation of highly localized polarons.[9−11] In addition, conjugated polymers incorporating alternating π-excessive and π-deficient aromatic moieties depicted significant decrease in their optical band gaps due to the introduction of intramolecular charge-transfer (ICT) structures and showed large third-order nonlinear optical susceptibility and interesting electrochemical properties.[12−18] These desirable properties afford the necessary motivation for further work toward the preparation of novel donor−acceptor materials.

Our research group has previously reported on the syntheses and characterization of the ABA type polymers poly[bis(3-alkylthienylenephenylene)] (PBTBC$_x$) based on electron-donating backbone structure.[19,20] In the work reported herein, we introduce an electron-accepting pyridinyl moiety in place of the phenylene unit in the polymer backbone with a view to investigate the properties of these novel donor−acceptor conjugated polymers. Although the polymers with this backbone structure have been reported in electrochemically generated systems,[21−23] little work has been done on the syntheses of these polymers using chemically grown polymers that are soluble and processable. Meanwhile, their physical properties such as thermal and optical properties have not been reported.

The reason pyridine is chosen as the electron-deficient moiety arises from its electron-deficient and acid-sensitive properties, which has been demonstrated to afford tunable electronic and optical properties in the derived polymers reported by others[21,26] and our group.[24,25] However, possibly arising from the introduction of the pyridinyl moiety between the functionalized thiophene rings, the widely used ferric chloride oxidation approach for polythiophene derivatives[27] could not achieve high molecular polymers. Here, we have used the Stille coupling approach for polymerization. We have also incorporated meta-linked pyridinyl moieties into polymer backbone (Scheme 1) for the purpose of investigating the structure−property correlation studies.

Experimental Section

Materials. The following reagents, 3-bromothiophene (Fluka, >95%), *N*-bromosuccinimide (Merck, 99%), Ni(dppp)Cl$_2$ (Fluka), 2,5-dibromopyridine (Fluka), 2,6-dibromopyridine (Fluka), 3,5-dibromopyridine (Fluka), 1-bromoalkane (Fluka), *n*-butyllithium (Merck, 1.6 M in hexane) and iodine (Fisher, 99%), were purchased from commercial sources and used without further purification, except Bu_4NBF_4 (TCI, for electrochemistry) which was dried under high vacuum before used. Chloroform (J.T. Baker) and acetonitrile (J.T. Baker) were reagent grade solvents and freshly distilled over calcium hydride. Tetrahydrofuran (J.T. Baker) and diethyl ether (J.T. Baker) were refluxed over metallic sodium wire/benzophenone for 4 h and distilled under a nitrogen atmosphere before used. 3-*n*-Hexylthiophene, 3-*n*-octylthiophene, 3-*n*-dodecylthiophene, 2-bromo-3-*n*-hexylthiophene, 2-bromo-3-*n*-octylthiophene, and 2-bromo-3-*n*-dodecylthiophene were synthesized according to the literature.[28]

* To whom correspondence should be addressed: Tel +65-6874-2922; Fax +65-6779-1691; e-mail chmngsc@leonis.nus.edu.sg.

10.1021/ma021082+ CCC: $25.00
Published on Web 02/08/2003

Scheme 1. Structures of Novel Conjugated Polymers

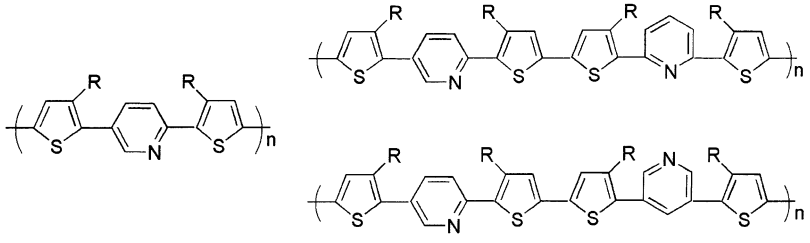

para-Linked polymers *meta*-Linked polymers

Instrumentation. Elemental analyses, mass spectra (MS), FTIR spectra, ^{1}H NMR and ^{13}H NMR spectra, UV and fluorescence spectra, scanning electron micrographs (SEM), thermogravimetric analysis (TGA), gel permeation chromatography analysis (GPC), and cyclic voltammetry (CV) were performed as previously reported.[25] Conductivity measurements were carried out on polymer pellets of known thickness using a four-point probe connected to a Keithley constant current source. XPS measurement of polymer powders was performed by means of a VG ESCA/SIMLAB MMKII with a Mg Kα radiation source (1253.6 eV). The binding energies were corrected for surface charging by referencing to the designated hydrocarbon C(1s) binding energy as 284.6 eV. Spectrum deconvolutions were carried out using the Gaussian component with the same full width at half-maximum (fwhm) for each component in a particular spectrum.

Synthesis. 2,5-Bis(3′-*n*-hexyl-2′-thienyl)pyridine (**5a**). 2-Bromo-3-*n*-hexylthiophene (6.05 g, 30 mmol) was slowly added to a suspension of magnesium turnings (0.84 g, 36 mmol) in 20 mL of dry THF at room temperature. The mixture was heated to reflux for 2 h. The produced Grignard reagent was transferred to a mixture of 2,5-dibromopyridine (3.54 g, 15 mmol) and Ni(dppp)Cl_2 (0.162 g, 0.3 mmol) suspended in 20 mL of THF at 0 °C dropwise. After the addition was finished, the mixture was allowed to warm to room temperature and heated to reflux for 24 h. The reaction mixture was quenched by ice water. The aqueous solution was neutralized by dilute hydrochloric acid and then extracted with diethyl ether (15 mL × 3). The organic layers were combined and washed with water and dried over magnesium sulfate. After filtration and concentration, the product was separated by column chromatography (silica gel, hexane and dichloromethylene as eluting solvent). The yield of **5a** was 50%. ^{1}H NMR ($CDCl_3$, ppm): δ = 8.70 (1H, d), 7.73 (1H, dd, J = 2.0 Hz), 7.57 (1H, d, J = 8.0 Hz), 7.30 (2H, t, J = 5.2 Hz), 7.02 (2H, d, J = 5.3 Hz), 2.94 (2H, t, J = 7.8 Hz), 2.70 (2H, t, J = 7.8 Hz), 1.64 (4H, m), 1.32 (12H, m), 0.87 (6H, t, J = 6.4 Hz). ^{13}C NMR: δ 151.94, 149.30, 140.97, 139.91, 136.68, 133.60, 130.70, 129.71, 128.34, 125.75, 124.58, 120.94, 31.76−14.00 (aliphatic Cs). FT-IR: 3108, 3068, 2959, 2926, 2855, 1590, 1556, 1468, 1435, 1384, 1361, 1292, 1229, 1090, 1028, 987, 964, 925, 889, 839, 768, 724, 693, 654. HR-MS: $C_{25}H_{33}NS_2$, Calcd: 411.2054; Found: 411.2034. Anal. Calcd: C, 72.96; H, 8.08; N, 3.40; S, 15.58. Found: C, 73.00; H, 8.76; N, 3.20; S, 15.28.

2,5-Bis(3′-*n*-octyl-2′-thienyl)pyridine (**5b**). The procedure of synthesis **5a** was repeated except that 2-bromo-3-*n*-octylthiophene was used instead of 2-bromo-3-*n*-hexylthiophene. Yield: 52%. ^{1}H NMR ($CDCl_3$, ppm): δ = 8.70 (1H, d), 7.73 (1H, dd, J = 2.4 Hz), 7.57 (1H, d, J = 8.0 Hz), 7.30 (2H, t, J = 5.2 Hz), 7.01 (2H, dd, J = 5.2 Hz), 2.92 (2H, t, J = 7.8 Hz), 2.68 (2H, t, J = 7.8 Hz), 1.67 (4H, m), 1.26 (20H, m), 0.87 (6H, t, J = 6.4 Hz). ^{13}C NMR: δ 151.96, 149.32, 140.97, 139.91, 136.68, 133.59, 130.70, 129.72, 128.35, 125.78, 124.58, 120.94, 31.80−14.00 (aliphatic Cs). FT-IR: 3108, 3068, 2959, 2924, 2854, 1590, 1557, 1476, 1435, 1378, 1366, 1292, 1229, 1153, 1096, 1028, 987, 964, 930, 884, 839, 768, 722, 693, 659. HR-MS: $C_{29}H_{41}NS_2$, Calcd: 467.2680; Found: 467.2684. Anal. Calcd: C, 74.48; H, 8.84; N, 3.00; S, 13.71. Found: C, 74.49; H, 8.94; N, 3.01; S, 12.78.

2,5-Bis(3′-*n*-dodecyl-2′-thienyl)pyridine (**5c**). The procedure of synthesis **5a** was repeated except that 2-bromo-3-*n*-dodecylthiophene was used instead of 2-bromo-3-*n*-hexylthiophene. Yield: 55%; mp: 42−44 °C. ^{1}H NMR ($CDCl_3$, ppm): δ = 8.70 (1H, d), 7.73 (1H, dd, J = 2.0 Hz), 7.57 (1H, d, J = 8.0 Hz), 7.30 (2H, t, J = 5.2 Hz), 7.01 (2H, dd, J = 5.2 Hz), 2.93 (2H, t, J = 7.8 Hz), 2.68 (2H, t, J = 7.8 Hz), 1.64 (4H, m), 1.25 (36H, m), 0.88 (6H, t, J = 6.4 Hz). ^{13}C NMR: δ 151.90, 149.22, 141.07, 139.94, 136.72, 133.54, 130.67, 129.70, 128.38, 125.78, 124.56, 120.98, 31.80−13.97 (aliphatic Cs). FT-IR: 3057, 2919, 2850, 1590, 1556, 1466, 1435, 1384, 1354, 1292, 1229, 1084, 1027, 987, 930, 884, 843, 734, 693, 653. HR-MS: $C_{37}H_{57}NS_2$, Calcd: 579.3933; Found: 579.3951. Anal. Calcd: C, 76.64; H, 9.91; N, 2.42; S, 11.06. Found: C, 76.25; H, 10.24; N, 2.55; S, 12.22.

2,6-Bis(3′-*n*-dodecyl-2′-thienyl)pyridine (**6**). The procedure of synthesis **5a** was repeated except that 2-bromo-3-*n*-dodecylthiophene and 2,6-dibromopyridine were used instead of 2-bromo-3-*n*-hexylthiophene and 2,5-dibromopyridine, respectively. Yield: 65%; mp: 39−40 °C. ^{1}H NMR ($CDCl_3$, ppm): δ = 7.70 (1H, t, J = 7.8 Hz), 7.40 (2H, d, J = 8.0 Hz), 7.29 (2H, d, J = 5.2 Hz), 6.99 (2H, d, J = 4.8 Hz), 3.00 (4H, t, J = 7.6 Hz), 1.69 (4H, m), 1.25 (36H, m), 0.88 (6H, t, J = 6.5 Hz). ^{13}C NMR: δ 152.99, 141.19, 137.63, 136.87, 130.71, 125.53, 118.90, 31.83−14.03 (aliphatic Cs). FT-IR: 2953, 2918, 2851, 1564, 1534, 1465, 1451, 1437, 1376, 1330, 1277, 1226, 1167, 1126, 944, 865, 832, 794, 755, 714, 671, 652, 638. HR-MS: $C_{37}H_{57}NS_2$, Calcd: 579.3933; Found: 579.3937. Anal. Calcd: C, 76.64; H, 9.91; N, 2.42; S, 11.06. Found: C, 76.17; H, 10.72; N, 3.04; S, 11.38.

3,5-Bis(3′-*n*-dodecyl-2′-thienyl)pyridine (**7**). The procedure of synthesis of **6** was repeated, except that 2-bromo-3-*n*-dodecylthiophene and 3,5-dibromopyridine were used instead of 2-bromo-3-*n*-hexylthiophene and 2,5-dibromopyridine, respectively. Yield: 64%. ^{1}H NMR ($CDCl_3$, ppm): δ = 8.64 (2H, s), 7.81 (1H, d), 7.34 (2H, d, J = 4.8 Hz), 7.04 (2H, d, J = 5.6 Hz), 2.70 (4H, t, J = 7.6 Hz), 1.60 (4H, m), 1.24 (36H, m), 0.88 (6H, t, J = 6.4 Hz). HR-MS: $C_{37}H_{57}NS_2$, Calcd: 579.3932; Found: 579.3941. Anal. Calcd: C, 76.64; H, 9.91; N, 2.42; S, 11.06. Found: C, 76.23; H, 10.21; N, 2.83; S, 11.54.

2,5-Bis(3′-*n*-hexyl-5′-iodo-2′-thienyl)pyridine (**8a**).[29] 2,5-Bis(3′-*n*-hexyl-2′-thienyl)pyridine (0.411 g, 1 mmol) was added to a two-neck 50 mL flask fitted with a magnetic stirrer and capped with a rubber septum. The system was vacuumed and flushed with nitrogen successively. Then, 15 mL of anhydrous ether was added via a syringe. The solution was cooled to −70 °C, and *n*-butyllithium (1.6 M in hexane) (1.31 mL, 2.10 mmol) was added dropwise by a syringe. The mixture was stirred at −70 °C for half an hour and then warmed to room temperature for a further hour and then cooled back to −70 °C; iodine solution (0.56 g, 2.19 mmol of I_2 in 20 mL of anhydrous ether) was added. After addition, the reaction mixture was allowed to warm to room temperature and kept for half an hour. The reaction was quenched by ice water. The aqueous solution was extracted with diethyl ether (15 mL × 3). The combined organic layers were washed with water and dried over magnesium sulfate. After filtration and concentration, the product was separated by column chromatography (silica gel, hexane as eluting solvent). Pure **8a** (0.55 g, 83% yield) is yellowish crystals; mp 37−38 °C. ^{1}H NMR ($CDCl_3$, ppm): δ = 8.59 (1H, d), 7.66 (1H, dd, J = 2.4 Hz), 7.46 (1H, d, J = 8.0 Hz), 7.15 (2H, d), 2.86 (2H, t, J = 7.8 Hz), 2.62 (2H, t, J = 7.8 Hz), 1.63 (4H, m), 1.32 (12H, m), 0.88 (6H, t, J = 6.4 Hz). ^{13}C

NMR: δ 151.21, 149.07, 143.47, 142.70, 141.97, 140.54, 139.47, 136.61, 127.54, 120.41, 75.59, 72.59, 31.52−14.00 (aliphatic Cs). FT-IR: 3010, 2954, 2920, 2846, 1652, 1583, 1553, 1517, 1479, 1468, 1415, 1377, 1279, 1225, 1162, 1109, 1025, 992, 961, 916, 827, 750, 723, 701, 618. HR-MS: $C_{25}H_{31}NS_2I_2$, Calcd: 662.9987; Found: 662.9984. Anal. Calcd: C, 45.25; H, 4.70; N, 2.11; S, 9.67; I, 38.25. Found: C, 45.22; H, 4.64; N, 2.18; S, 10.35; I, 38.35.

2,5-Bis(3′-*n*-octyl-5′-iodo-2′-thienyl)pyridine (8b). The procedure of synthesis **8a** was repeated except that 2,5-bis(3′-*n*-octyl-2′-thienyl)pyridine was used instead of 2,5-bis(3′-*n*-hexyl-2′-thienyl)pyridine. Yield: 85%; mp: 47.5−49.0 °C. ^{1}H NMR ($CDCl_3$, ppm): δ = 8.60 (1H, d), 7.66 (1H, dd, J = 2.4 Hz), 7.46 (1H, d, J = 8.0 Hz), 7.13 (2H, d), 2.86 (2H, t, J = 7.8 Hz), 2.62 (2H, t, J = 7.8 Hz), 1.63 (4H, m), 1.32 (20H, m), 0.87 (6H, t, J = 6.4 Hz). ^{13}C NMR: δ 151.22, 149.07, 143.45, 142.70, 141.97, 140.52, 139.45, 136.61, 127.52, 120.41, 75.60, 72.59, 31.82−14.02 (aliphatic Cs). FT-IR: 3025, 2950, 2919, 2847, 1665, 1588, 1549, 1462, 1422, 1374, 1275, 1221, 1188, 1118, 1082, 1032, 995, 927, 907, 883, 837, 765, 747, 723, 706, 675. HR-MS: $C_{29}H_{39}NS_2I_2$, Calcd: 719.0613; Found: 719.0620. Anal. Calcd: C, 48.41; H, 5.46; N, 1.95; S, 8.91; I, 35.27. Found: C, 48.51; H, 5.31; N, 2.10; S, 9.50; I, 33.18.

2,5-Bis(3′-*n*-dodecyl-5′-iodo-2′-thienyl)pyridine (8c). The procedure of synthesis of **8a** was repeated except that 2,5-bis(3′-*n*-dodecyl-2′-thienyl)pyridine was used instead of 2,5-bis(3′-*n*-hexyl-2′-thienyl)pyridine. Yield: 86%; mp: 60.0−61.0 °C. ^{1}H NMR ($CDCl_3$, ppm): δ = 8.60 (1H, d), 7.66 (1H, dd, J = 2.4 Hz), 7.46 (1H, d, J = 8.4 Hz), 7.15 (2H, d), 2.86 (2H, t, J = 7.8 Hz), 2.61 (2H, t, J = 7.8 Hz), 1.60 (4H, m), 1.25 (36H, m), 0.87 (6H, t, J = 6.4 Hz). ^{13}C NMR: δ 151.22, 149.08, 143.47, 142.73, 141.98, 140.55, 139.53, 139.48, 136.54, 127.55, 120.40, 75.60, 72.59, 31.82−14.02 (aliphatic Cs). FT-IR: 2920, 2848, 1651, 1557, 1461, 1424, 1373, 1030, 832, 723, 673. HR-MS: $C_{37}H_{55}NS_2I_2$, Calcd: 831.1865; Found: 831.1853. Anal. Calcd: C, 53.43; H, 6.67; N, 1.68; S, 7.71; I, 30.51. Found: C, 53.79; H, 6.72; N, 1.56; S, 8.19; I, 30.08.

2,6-Bis(3′-*n*-dodecyl-5′-iodo-2′-thienyl)pyridine (10). The procedure of synthesis of **8a** was repeated except that 2,6-bis(3′-*n*-dodecyl-2′-thienyl)pyridine was used instead of 2,5-bis(3′-*n*-hexyl-2′-thienyl)pyridine. Yield: 83%; mp: 34.0−36.0 °C. ^{1}H NMR ($CDCl_3$, ppm): δ = 7.69 (1H, t, J = 7.8 Hz), 7.28 (2H, dd, J = 8.0 Hz), 7.11 (2H, s), 2.88 (4H, t, J = 7.8 Hz), 1.65 (4H, m), 1.25 (36H, m), 0.88 (6H, t, J = 6.4 Hz). ^{13}C NMR: δ 151.93, 142.79, 140.57, 137.10, 118.53, 75.42, 31.82−14.01 (aliphatic Cs). FT-IR: 2958, 2922, 2849, 1563, 1532, 1457, 1427, 1268, 1170, 1068, 825, 795, 726, 699, 664, 618. HR-MS: $C_{37}H_{55}NS_2I_2$, Calcd: 831.1865; Found: 831.1847. Anal. Calcd: C, 53.43; H, 6.67; N, 1.68; S, 7.71; I, 30.51. Found: C, 53.68; H, 6.90; N, 1.85; S,8.01; I, 29.89.

3,5-Bis(3′-*n*-dodecyl-5′-iodo-2′-thienyl)pyridine (11). The procedure of synthesis of **6a** was repeated except that 3,5-bis(3′-*n*-dodecyl-2′-thienyl)pyridine was used instead of 2,5-bis(3′-*n*-hexyl-2′-thienyl)pyridine. Yield: 80%; mp: 43.0−45.5 °C. ^{1}H NMR ($CDCl_3$, ppm): δ = 8.58 (2H, s), 7.64 (1H, s), 7.16 (2H, s), 2.61 (4H, t, J = 7.8 Hz), 1.55 (4H, m), 1.25 (36H, m), 0.88 (6H, t, J = 6.4 Hz). FT-IR: 3040, 2954, 2916, 2849, 1589, 1541, 1468, 1403, 1374, 1312, 1276, 1216, 1154, 1077, 1024, 923, 882, 837, 766, 718, 691, 672, 638. HR-MS: $C_{37}H_{55}NS_2I_2$, Calcd: 831.1865; Found: 831.1847. Anal. Calcd: C, 53.43; H, 6.67; N, 1.68; S, 7.71; I, 30.51. Found: C, 53.67; H, 6.68; N, 1.63; S, 8.36; I, 30.18.

2,5-Bis(3′-*n*-hexyl-5′-tributylstannyl-2′-thienyl)pyridine (9a). 2,5-Bis(3′-*n*-hexyl-2′-thienyl)pyridine (0.411 g, 1 mmol) was dissolved in 15 mL of dry anhydrous ether in a 50 mL flask, which was fitted with a magnetic stirrer and rubber septum under a N_2 atmosphere. *n*-Butyllithium (1.6 M in hexane) (1.31 mL, 2.10 mmol) was added via a syringe at −70 °C. After the mixture was stirred for 30 min and then warmed to room temperature for 30 min, the resulting solution gradually became an orange suspension. The mixture was then cooled back to −70 °C, and tributyltin chloride (0.683 g, 2.10 mmol) was added. The solution was gradually warmed to room temperature, stirred for 1 h, and then hydrolyzed by ice water. The separated organic phase was dried over anhydrous magnesium sulfate. The solvent was evaporated by vacuum distillation, and a yellow viscous liquid was obtained. The yield was 87%. ^{1}H NMR ($CDCl_3$, ppm): δ = 8.71 (1H, d), 7.72 (1H, dd, J = 2.2 Hz), 7.54 (1H, d, J = 8.4 Hz), 7.02 (2H, d), 2.93 (2H, t, J = 7.8 Hz), 2.70 (2H, t, J = 7.8 Hz), 1.60−0.90 (76H, m). ^{13}C NMR: δ 151.80, 148.97, 142.85, 141.68, 140.81, 139.28, 138.33, 137.91, 136.27, 128.42, 120.61, 31.81−10.68 (aliphatic Cs). FT-IR: 3036, 2956, 2924, 2853, 1663, 1589, 1554, 1531, 1459, 1418, 1377, 1340, 1292, 1244, 1178, 1152, 1073, 1023, 960, 930, 875, 839, 767, 692, 663, 598, 504. Anal. Calcd for $C_{49}H_{85}NS_2Sn_2$: C, 59.46; H, 8.65; N, 1.42; S, 6.48. Found: C, 60.08; H, 8.76; N, 1.57; S, 6.54.

2,5-Bis(3′-*n*-octyl-5′-tributylstannyl-2′-thienyl)pyridine (9b). The procedure of synthesis of **9a** was repeated except that 2,5-bis(3′-*n*-octyl-2′-thienyl)pyridine was used instead of 2,5-bis(3′-*n*-hexyl-2′-thienyl)pyridine. Yield: 88%. ^{1}H NMR ($CDCl_3$, ppm): δ = 8.70 (1H, d), 7.75 (1H, dd, J = 2.0 Hz), 7.51 (1H, d, J = 7.9 Hz), 7.02 (2H, d), 2.92 (2H, t, J = 7.8 Hz), 2,70 (2H, t, J = 7.8 Hz), 1.60−0.90 (84H, m). ^{13}C NMR: δ 151.80, 148.97, 142.83, 141.68, 140.81, 139.28, 138.34, 137.91, 136.29, 128.42, 120.62, 31.81−10.68 (aliphatic Cs). FT-IR: 3036, 2956, 2924, 2853, 1664, 1589, 1555, 1531, 1459, 1418, 1377, 1340, 1292, 1244, 1178, 1152, 1073, 1023, 960, 930, 875, 839, 767, 692, 663, 598, 504. Anal. Calcd for $C_{53}H_{93}NS_2Sn_2$: C, 60.87; H, 8.96; N, 1.34; S, 6.13. Found: C, 61.12; H, 9.31; N, 1.56; S, 6.50.

2,5-Bis(3′-*n*-dodecyl-5′-tributylstannyl-2′-thienyl)pyridine (9c). The procedure of synthesis of **9a** was repeated except that 2,5-bis(3′-*n*-dodecyl-2′-thienyl)pyridine was used instead of 2,5-bis(3′-*n*-hexyl-2′-thienyl)pyridine. Yield: 90%. ^{1}H NMR ($CDCl_3$, ppm): δ = 8.70 (1H, d), 7.72 (1H, dd, J = 2.4 Hz), 7.51 (1H, d, J = 8.4 Hz), 7.02 (2H, d), 2.92 (2H, t, J = 7.8 Hz), 2.70 (2H, t, J = 7.8 Hz), 1.60−0.91 (100H, m).^{13}C NMR: δ 151.80, 148.95, 142.85, 141.68, 140.80, 139.40, 139.28, 138.34, 136.27, 128.42, 120.61, 63.24, 31.52−10.67 (aliphatic Cs). FT-IR: 3030, 2956, 2924, 2853, 1663, 1589, 1555, 1531, 1464, 1418, 1377, 1340, 1292, 1244, 1179, 1152, 1073, 1018, 960, 930, 872, 840, 767, 692, 663, 599, 504. Anal. Calcd for $C_{61}H_{109}NS_2Sn_2$: C, 63.27; H, 9.49; N, 1.21; S, 5.54. Found: C, 63.85; H, 9.58; N, 1.33; S, 5.43.

General Procedure for Polymerization. 2,5-Bis(3′-*n*-alkyl-5′-tributylstannyl-2′-thienyl)pyridine (1.5 mmol), 2,5-bis(3′-*n*-alkyl-5′-iodo-2′-thienyl)pyridine (1.5 mmol), and tetrakis(triphenylphosphino)palladium(0) (0.03 mmol) were placed in a 100 mL two-neck, round-bottomed flask and deareated with nitrogen. Thereafter, THF (60 mL) was syringed into the reaction flask. This reaction mixture was stirred and refluxed for 5 days. The reaction mixture was concentrated to 10 mL by vacuum distillation and poured into 400 mL of methanol. The precipitated polymer was collected by filtration and further purified by redissolving in chloroform and precipitating into methanol. The resulting polymer was washed with methanol for 24 h and with acetone for 12 h and finally extracted with chloroform through a Soxhlet apparatus. The polymer was obtained by concentrating the solution and subsequent precipitation into methanol.

Poly[(3′-*n*-hexylthiophene-2′,5′-diyl)(pyridine-2,5-diyl)-(3′-*n*-hexylthiophene-2′,5′-diyl)] (12a). Yield: 68%. ^{1}H NMR ($CDCl_3$, ppm): δ 8.73 (br, pyridinyl proton, 1H), 7.76 (br peaks, pyridinyl proton, 1H), 7.61 (br peaks, pyridinyl proton, 1H), 7.17 (br peaks, thiophenyl proton, 2H), 2.93 (br, −thiophenyl−CH_2−, 2H), 2.69 (br, −thiophenyl−CH_2−, 2H), 1.68−0.89 (m, −$(CH_2)_4CH_3$). FT-IR: 2922, 2854, 1700, 1651, 1558, 1541, 1459, 1370, 1367, 1270, 1034, 920, 824, 668. Anal. Calcd for $(C_{25}H_{31}NS_2)_n$: C, 73.38; H, 7.63; N, 3.42; S, 15.65. Found: C, 69.34; H, 8.19; N, 3.42; S, 13.37; I, 1.50.

Poly[(3′-*n*-octylthiophene-2′,5′-diyl)(pyridine-2,5-diyl)-(3′-*n*-octylthiophene-2′,5′-diyl)] (12b). Yield: 70%. ^{1}H NMR ($CDCl_3$, ppm): δ 8.73 (br, pyridinyl proton, 1H), 7.76 (br peaks, pyridinyl proton, 1H), 7.61 (br peaks, pyridinyl proton, 1H), 7.16 (br peaks, thiophenyl proton, 2H), 2.92 (br, −thiophenyl−CH_2−, 2H), 2.69 (br, −thiophenyl−CH_2−, 2H), 1.72−0.87 (m, −$(CH_2)_6CH_3$). FT-IR: 2921, 2852, 1700, 1651, 1558, 1548, 1463,

Scheme 2. Synthetic Scheme to Monomers 5, 6, and 7[a]

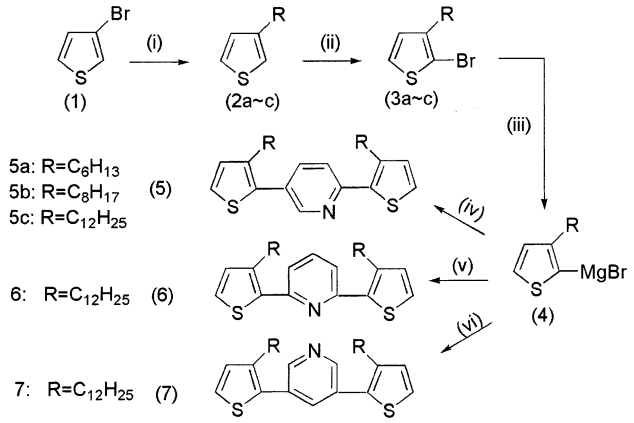

[a] Reagents and conditions: (i) RMgBr, Et_2O, Ni(dppp)Cl_2; (ii) NBS/AcOH/$CHCl_3$; (iii) Mg, Et_2O; (iv) 2,5-dibromopyridine, Ni(dppp)Cl_2; (v) 2,6-dibromopyridine, Ni(dppp)Cl_2; (vi) 3,5-dibromopyridine, Ni(dppp)Cl_2.

1371, 1270, 1023, 921, 824, 716, 663. Anal. Calcd for $(C_{29}H_{39}NS_2)_n$: C, 74.78; H, 8.44; N, 3.01; S, 13.77. Found: C, 71.66; H, 8.32; N, 2.70; S, 12.45; I, 3.37.

Poly[(3′-*n*-dodecylthiophene-2′,5′-diyl)(pyridine-2,5-diyl)(3′-*n*-dodecylthiophene-2′,5′-diyl)] (**12c**). Yield: 65%. ^{1}H NMR ($CDCl_3$, ppm): δ 8.73 (br, pyridinyl proton, 1H), 7.76 (br peaks, pyridinyl proton, 1H), 7.60 (br peaks, pyridinyl proton, 1H), 7.16 (br peaks, thiophenyl proton, 2H), 2.91 (br, −thiophenyl−CH_2−, 2H), 2.69 (br, −thiophenyl−CH_2−, 2H), 1.68−0.87 (m, −$(CH_2)_{10}CH_3$). FT-IR: 2919, 2850, 1650, 1548, 1467, 1371, 1271, 1217, 1071, 1023, 921, 825, 717, 663. Anal. Calcd for $(C_{37}H_{55}NS_2)_n$: C, 76.89; H, 9.59; N, 2.42; S, 11.09. Found: C, 71.96; H, 8.38; N, 1.78; S, 10.11; I, 3.55.

Poly[(3′-*n*-dodecylthiophene-2′,5′-diyl)(pyridine-2,5-diyl)(3′-*n*-dodecylthiophene-2′,5′-diyl)-*co*-*alt*-(3′-*n*-dodecylthiophene-2′,5′-diyl)(pyridine-2,6-diyl)(3′-*n*-dodecylthiophene-2′,5′-diyl)] (**13**). The procedure of synthesis **12c** was repeated except that 2,6-bis(3′-*n*-dodecyl-5′-iodo-2′-thienyl)pyridine (**10**) was used instead of 2,5-bis(3′-*n*-dodecyl-5′-iodo-2′-thienyl)pyridine (**8c**). Yield: 70%. ^{1}H NMR ($CDCl_3$, ppm): δ 8.73, 7.71, 7.60, 7.40, 7.15, 7.10, 2.93, 2.69, 1.68−0.89. FT-IR: 2923, 2852, 1652, 1559, 1457, 1357, 1158, 829, 716, 663. Anal. Calcd for $(C_{37}H_{55}NS_2)_n$: C, 76.89; H, 9.59; N, 2.42; S, 11.09. Found: C, 72.71; H, 9.42; N, 3.23; S, 11.33; I, 2.25.

Poly[(3′-*n*-dodecylthiophene-2′,5′-diyl)(pyridine-2,5-diyl)(3′-*n*-dodecylthiophene-2′,5′-diyl)]-*co*-*alt*-(3′-*n*-dodecylthiophene-2′,5′-diyl)(pyridine-3,5-diyl)(3′-*n*-dodecylthiophene-2′,5′-diyl)] (**14**). The procedure of synthesis of **12c** was repeated, except that 3,5-bis(3′-*n*-dodecyl-5′-iodo-2′-thienyl)pyridine (**11**) was used instead of 2,5-bis(3′-*n*-dodecyl-5′-iodo-2′-thienyl)pyridine (**8c**). Yield: 75%. ^{1}H NMR ($CDCl_3$, ppm): δ 8.73, 8.67, 7.84, 7.79, 7.61, 7.20, 7.11, 2.93, 2.69, 1.68−0.89. FT-IR: 2923, 2852, 1652, 1558, 1541, 1460, 1373, 1021, 828, 716. Anal. Calcd for $(C_{37}H_{55}NS_2)_n$: C, 76.89; H, 9.59; N, 2.42; S, 11.09. Found: C, 76.32; H, 9.94; N, 2.35; S, 9.80; I, 0.35.

Results and Discussion

Synthesis of the Polymers. The synthesis of bis-(2-thienyl)pyridines (**5a**−**c**, **6**, and **7**) was achieved using Grignard coupling reactions, as shown in Scheme 2. 2-Bromo-3-*n*-alkylthiophenes (**3**) were reacted with magnesium to afford the corresponding Grignard reagents, which were then coupled with dibromopyridine in the presence of a catalytic amount of Ni(dppp)Cl_2 to afford compounds **5**−**7**. Then, **5**−**7** were reacted with *n*-butyllithium at −70 °C, followed by treatment with tributyltin chloride or iodination to give compounds

Scheme 3. Synthetic Approach to Polymers with 2,5-Pyridinyl Linkages[a]

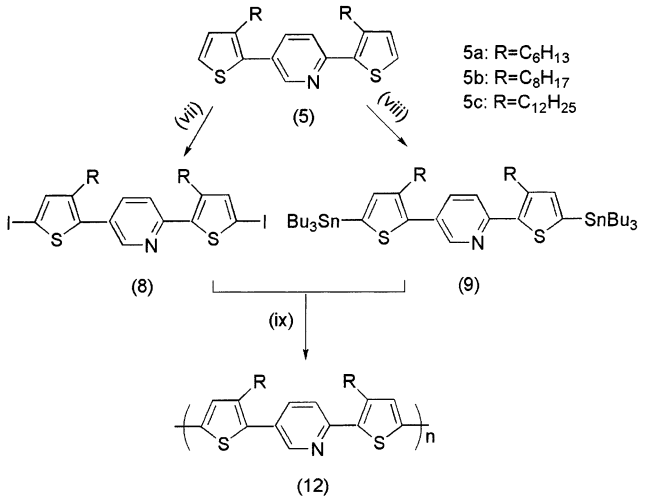

[a] Reagents and conditions: (vii) ^{n}BuLi, Et_2O, and then I_2; (viii) ^{n}BuLi, Et_2O, Bu_3SnCl, −70 °C; (ix) $Pd(PPh_3)_4$/THF/Δ.

9a−**c** and **8a**−**c**, **10**, and **11**, respectively (Scheme 3 and Scheme 4).

Compounds **5**−**11** showed different physical properties due to the different substituents or backbones. **5a** and **5b** were orange viscous liquids with strong fluorescence under UV light. **7** was a brown liquid with weak fluorescence. The other two compounds **5c** and **6** were light yellow solids. Compounds **9a**−**c** were light yellow viscous liquids, and all diiodo-substituted compounds (**8a**−**c**, **10**, and **11**) were yellow crystals. The structure and purity of these monomers were confirmed by NMR (^{1}H and ^{13}C), HR-MS, and elemental analyses as reported in the Experimental Section.

Polymerization was carried out in THF in the presence of catalytic amounts (ca. 2 mol %) of $Pd(PPh_3)_4$ under a nitrogen atmosphere. When the reaction ended, the polymer was precipitated into methanol and subjected to Soxhlet extractions to eliminate oligomers. Purification was carried out by dissolving polymer in $CHCl_3$ and then reprecipitation in methanol. All polymerizations were carried out smoothly with good yields. The results are summarized in Table 1.

Polymer Physical Properties. The derived polymers with pyridinyl moieties having meta vs para linkages depicted different physical properties. **12a**−**c** with *p*-pyridinyl linkages were red powders, while **13** and **14** with meta-linkages were red resins. All polymers have good solubility in organic solvents such as tetrahydrofuran, dichloromethylene, and chloroform as well as trifluoroacetic acid and formic acid.

The structures of the derived polymers were characterized by spectroscopic methods. The spectral assignments clearly corroborated the proposed structure. For polymers **12a**−**c**, similar characteristic chemical shifts were observed in ^{1}H NMR spectra. Figure 1 showed ^{1}H NMR spectra of the representative polymer **12b** in comparison with monomer **5b**. The chemical shifts of the pyridinyl protons of **12b** were manifested at δ 8.73, 7.76, and 7.61 ppm while the C_β-proton of the thiophene ring appeared at 7.16 ppm. The remaining resonance at δ 2.92, 2.69, and 1.72−0.87 ppm can be correlated to the octyl pendant chains on thienylene unit. Polymers **13** and **14** containing para- and meta-linked pyridinyl moieties depicted more complicate NMR spectra com-

Scheme 4. Synthetic Approach to Polymers with *m*-Pyridinyl Linkages[a]

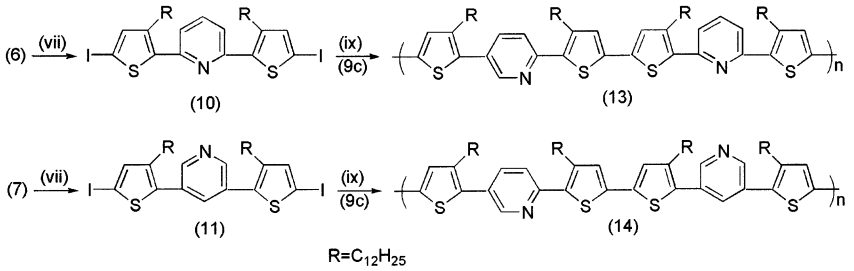

[a] Reagents and conditions: (vii) ^{n}BuLi, Et_2O, and then I_2; (viii) ^{n}BuLi, Et_2O, Bu_3SnCl, −70 °C; (ix) $Pd(PPh_3)_4$/THF/Δ.

Table 1. Synthetic Yield and Physical Properties of Polymers

		GPC results				conductivity/S cm^{-1}	
polymer	yield (%)	$M_n \times 10^{-3}$	$M_w \times 10^{-3}$	PDI	n[a]	I^2-doped	$FeCl_3$-doped
12a	68	5.4	8.6	1.59	39	8.75×10^{-5}	3.16×10^{-4}
12b	70	6.7	12.0	1.80	45	2.79×10^{-5}	8.26×10^{-5}
12c	65	5.7	7.8	1.36	27	8.42×10^{-6}	
13	70	10.6	15.4	1.46	54	*b*	*b*
14	75	12.7	21.6	1.71	66	*b*	*b*

[a] Number of aromatic rings. [b] The pellets of the polymers are difficult to compress.

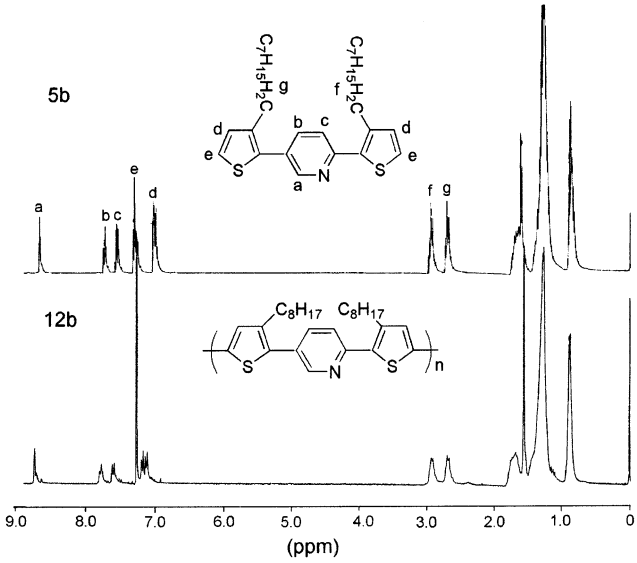

Figure 1. ^{1}H NMR spectra of the representative polymer **12b** in comparison to compound **5b**.

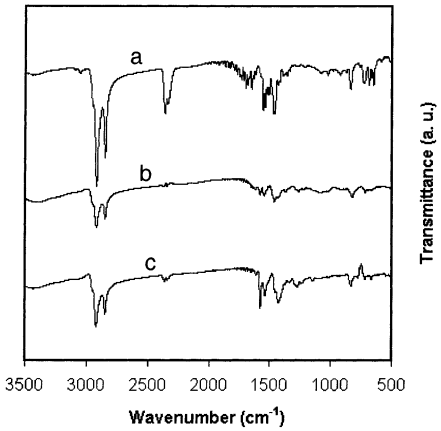

Figure 2. IR spectra of polymer **12c**: (a) the neutral polymer; (b) $FeCl_3$-doped polymer; (c) I_2-doped polymer.

pared to **12c** due to the different chemical environments of the protons on the thienylene and pyridine units within the polymer backbone. FT-IR spectra of the polymers are consistent with the expected structures. Elemental analyses of the novel polymers are within range of the expected formula.

The molecular weights of polymers were determined by GPC using THFas eluant and polystyrene as standard. The results are summarized in Table 1. The novel polymers had a number-average weight (M_n) ranging from 5.4 to 12.7 kDa with polydispersity (PDI) from 1.36 to 1.80, corresponding to the presence of 27−66 aromatic rings. Meta-linked polymers **13** and **14** showed higher molecular weights compared to para-linked ones.

When doped with I_2 and $FeCl_3$, the derived polymers were electrically conductive. The conductivity of the polymers **12a**−**c** in their doped states were of the order of 10^{-6}−10^{-4} S cm^{-1}, which is lower than that of ABA type $PBTBC_x$.[19,20] All measurement results are listed in Table 1. It is apparent that the conductivities of the polymers decrease with increasing substituted chain length. This correlated to the observation in the study of $PBTBC_x$[20] and poly(alkylthiophene)s.[30]

The doped polymers showed a dramatic change in their FTIR spectra (Figure 2). The stretching vibrations in the region of 1000−1500 cm^{-1} became broad due to the positively charged state of the polymer backbone. The relative intensities of the stretchings are all greatly reduced because of "the rise of the baseline" as a result of the enhanced absorption in IR region due to the formation of polarons and bipolarons.[23]

Thermal Properties of the Polymers. The polymer thermal stability was evaluated using TGA under either a nitrogen or air atmosphere. Polymers **12a**−**c** showed similar thermal stability, as minimal weight change (<10%) was observed on heating to 420 °C in air and a nitrogen atmosphere. In a nitrogen atmosphere, an apparently one-step degradation mainly attributable to the cleavage of pendant group and partial decomposition of backbone was observed. The amount of residues decrease with increasing alkyl chain length, which is consistent with degradation of pendant chains of increasing bulkiness. The degradation of the polymers in air depicted a two-step decomposition pattern, corresponding to the cleavage of the alkyl chain and the subsequent degradation of the polymer chain.

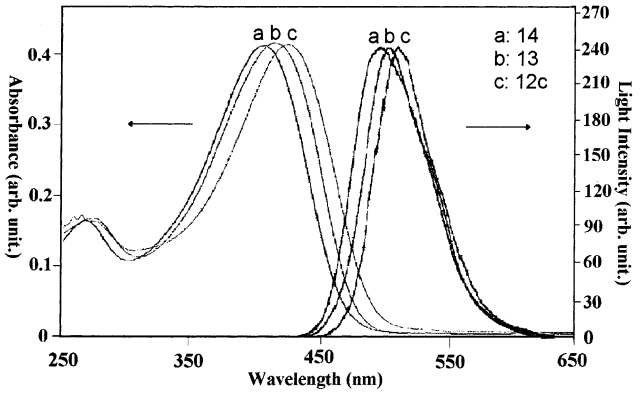

Figure 3. UV−vis absorption and fluorescence spectra of the polymers with different linked backbones in $CHCl_3$ solution.

Meta-linked polymers **13** and **14** depicted better thermal stability with both of them exhibiting an onset of degradation greater than 300 °C in N_2 and air, and polymer **14** containing 3,5-pyridinyl units showed the highest degradation onset temperature (440 °C) in those.

Optical Properties of Polymers. *Optical Properties in Solution.* The UV−vis absorption and fluorescence emission spectra of polymers in solution phase were recorded in dilute chloroform and trifloroacetic acid at room temperature.

The optical properties of the derived polymers in $CHCl_3$ solution are mainly dependent on pyridinyl linked patterns of their backbones. Polymers **12a**−**c** with 2,5-linked pyridinyl units depicted almost identical behavior in optical absorption and emission spectra. The absorption spectra exhibited a single absorption peak (λ_{max}) at 429−432 nm. The PL spectra were obtained by excitation at the absorption maxima. Polymers **12a**−**c** afforded a strong green fluorescence with emission maxima at 511−513 nm, which were roughly at the onset positions of their absorption band.

As to polymers **13** and **14** containing meta-linked pyridinyl units, the absorption and emission maxima were blue-shifted in comparison to **12a**−**c**. This might be attributed to the lesser extent of π-electron delocalization of the polymer main chain arising from meta-linkages, causing a reduction of the π-conjugation lengths. Polymer **14** containing 3,5-linked pyridinyl units depicted the highest energy transitions in the UV and fluorescence spectra, implying the least mean conjugation length. Figure 3 depicted the UV−vis absorption and fluorescence spectra of polymers **12c**, **13**, and **14** in $CHCl_3$ solution.

The fluorescent quantum yield in solution was determined according to the method described previously[25] relative to quinine sulfate in 0.1 N H_2SO_4. The results are summarized in Table 2. The fluorescent quantum yields of the novel polymers were higher than that of poly(3-alkylthiophene)s[31] and $PBTBC_x$.[19]

For the purpose of comparison, we have measured the optical properties of the derived polymers in CF_3COOH solution. Like other soluble conjugated polymers containing pyridinyl[32,25] or quinoline units,[33] the derived polymers showed UV absorption maxima and emission peaks at a longer wavelength in CF_3COOH solution than in $CHCl_3$ solution. This indicates that the absorption and emission of these polymers are strongly affected by the protonation of nitrogen, which cause distortion of the bonds connecting the neighboring units due to accentuated steric repulsion.[33] Interestingly, the polymers depicted nearly identical emission peaks at ca. 548 nm (greenish-yellow) in CF_3COOH solution although they have different backbones and different UV absorption maxima.

The excitation spectra of polymers were obviously different when using $CHCl_3$ and CF_3COOH as solvents (see Table 2). In $CHCl_3$ solution, the excitation curves of all polymers are closely to their UV absorption curves, as often observed in polymers soluble in common organic solution. However, when emitted at 548 nm in CF_3COOH solution, the excitation maxima of all polymers were shifted to longer wavelength. Figure 4 showed the UV−vis absorption, excitation, and emission curves of polymers **12c**, **13**, and **14** in CF_3COOH solutions.

Optical Properties in Film Phase. All novel polymers are easily spin-coated onto glass substrates to afford highly transparent, pinhole-free films. The film of polymers **12a**−**c** showed $\pi-\pi^*$ absorption maxima at about 449 nm. Similarly, polymer **13** and **14** depicted blue-shifted absorption maxima in the film state in comparison to polymers **12a**−**c** for the same reason mentioned for polymers in solution. The polymers in the film phase depicted a red shift of about 20−30 nm from their solutions, which could be ascribed to conformational changes increasing the degree of conjugation in the polymer backbone of the condensed state.[31] However, this bathochromic shift is somewhat less than that observed for poly(3-alkylthiophene)s in the range 60−100 nm,[31] suggesting that the introduction of pyridinyl unit imparted a significant amount of rigidity to the polymer backbone. The band gap energy of the polymers deduced from the energy absorption edge of the UV−vis spectrum according to the approach of Johnson et al.[34] was about 2.34, 2.39, and 2.46 eV for polymers **12a**−**c**, **13**, and **14**, respectively.

The temperature-dependent absorption of the polymer was studied in film phases. Figure 5 depicts the representative spectra for polymers **12c**, **13**, and **14**. For polymer **12c**, the absorption maximum (449 nm) underwent a blue shift with gradual decrease in the intensity with increasing temperature, while a new band (288 nm) appeared with increasing intensity. This indicates a decrease of the conjugation length. This observation is due to heat-induced disorder in the side chain leading to accentuated steric interaction and concomitant twisting of the polymer chain, reducing the extent of inter-ring conjugation.[35] The magnitude of the blue shift is significantly lesser in comparison to poly(alkylthiophene)s,[35] indicating that the extent of twisting of the polymer chain is very much reduced. This might be due to the spacer effect of the pyridinyl unit on the polymer chain, which helps diminish the repulsive intrachain steric interactions exerted by the alkyl pendant groups. It should also be noted that one isosbestic point is observed in UV spectra, implying the coexistence of two different phases. The isosbestic point would imply the presence of some cooperative effects in the simultaneous rotation of long sequences of polymer repeat units.[36]

Other polymers exhibited similar behavior in their UV spectra upon heating. From Figure 5, the three polymers which have the same substituents but different linkages in the backbone, the same new band (288 nm) with increasing intensity in their UV spectra was observed upon heating. This thermochromic behavior

Table 2. Optical Properties of the Derived Polymers in Solution and Film States

	solution state									
	In $CHCl_3$ solution				in CF_3COOH solution			film state[d]		
polymer	UV λ_{max} (nm)	Ex[a] λ (nm)	Em[b] λ_{max} (nm)	φ[c]	UV λ_{max} (nm)	Ex[a] λ (nm)	Em[b] λ_{max} (nm)	UV λ_{max} (nm)	Em λ_{max} (nm)	E_g[e] (eV)
12a	432	431	513	43.8	465	479	548	459	540	2.34
12b	432	432	514	42.3	472	480	549	458	540	2.34
12c	429	429	511	40.3	474	479	548	449	541	2.34
13	414	414	503	42.8	464	492	548	443	534	2.46
14	407	407	500	37.2	453	492	548	424	528	2.39

[a] Ex = excitation. Emitted by emission maxima. [b] Em = emission. Excited by UV maxima. [c] φ = quantum yield. Relative to 10^{-5} M quinine sulfate in 0.1 N H_2SO_4 solution. [d] Films were obtained by spin-coating from $CHCl_3$ solution. [e] E_g = band gap.

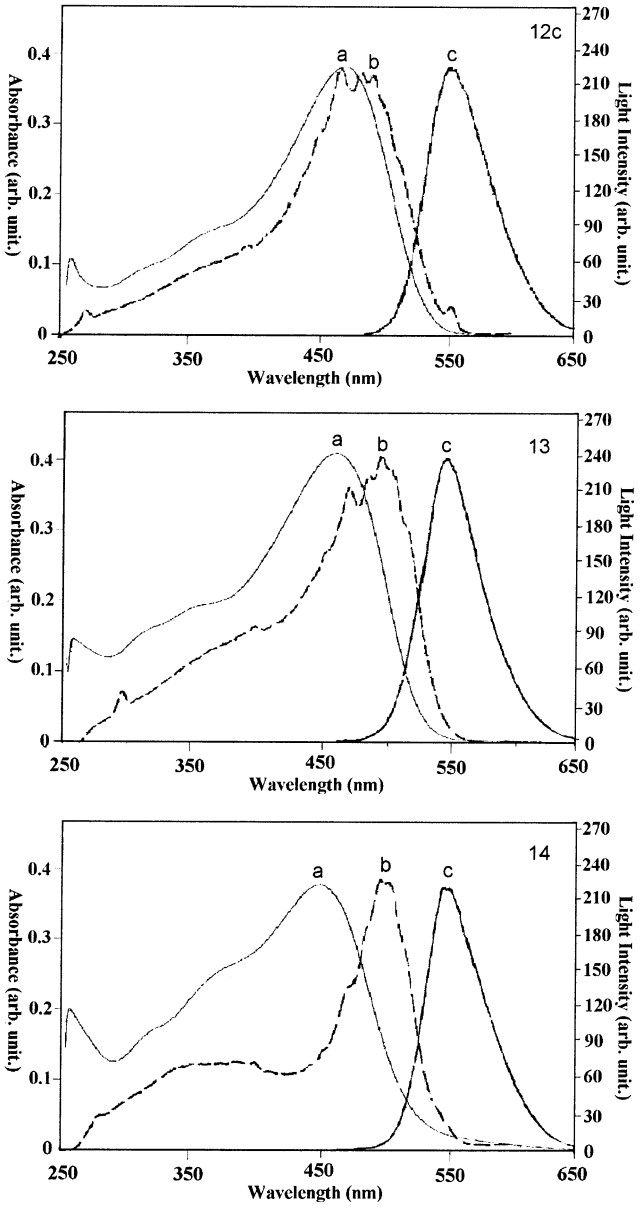

Figure 4. (a) UV absorption, (b) excitation, and (c) emission curves of polymers **12c**, **13**, and **14** in CF_3COOH solution.

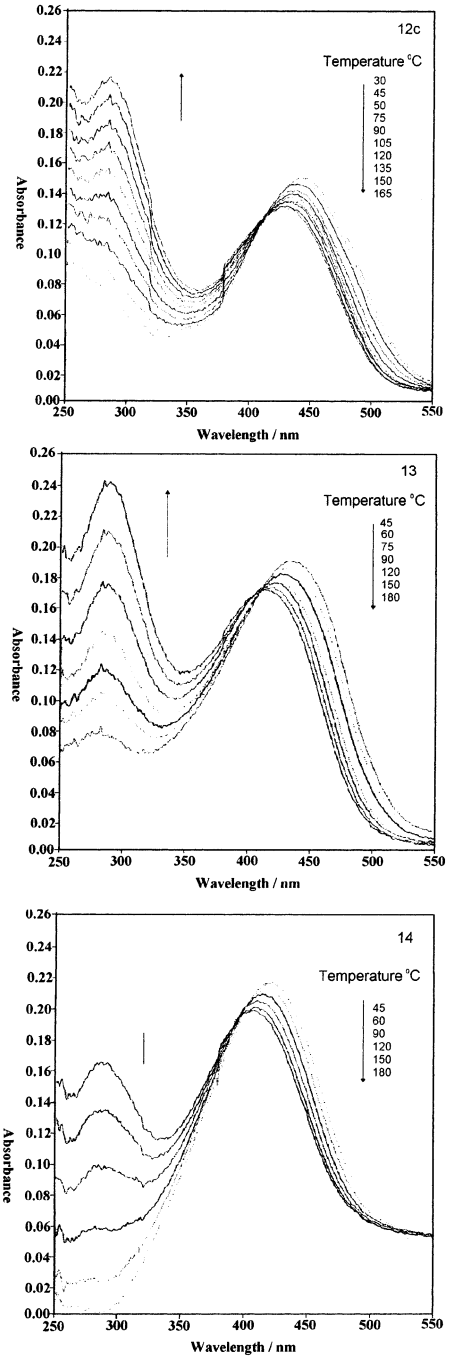

Figure 5. Variation of absorption maxima in UV−vis spectra of polymers **12c**, **13**, and **14** upon heating in film states.

was reversible, regaining the initial absorption state upon cooling.

The emission maxima (upon excitation at absorption maxima) of the derived polymers occurred in the green region at ca. 540 nm for **12a**−**c** and 534 and 528 nm for **13** and **14**, respectively. Similarly, polymer with meta-linked backbone exhibited a blue shift from those with para-linked analogues. Polymer **14** with 3,5-pyridinyl units depicted the shortest emission wavelength. The optical properties of polymer films are summarized in

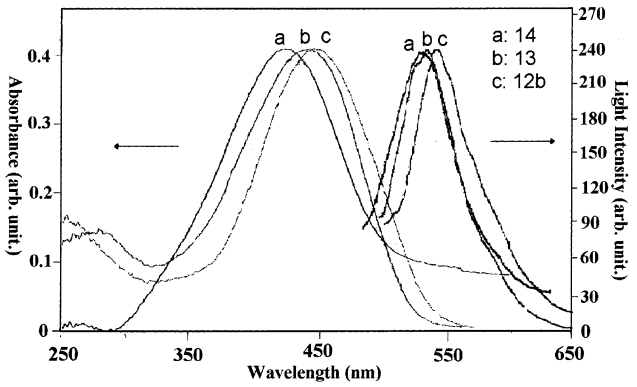

Figure 6. UV−vis absorption and photoluminescence spectra of the polymer films on ITO glass.

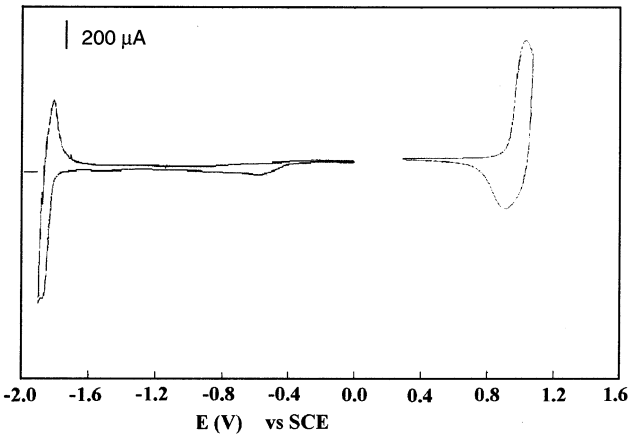

Figure 7. Cyclic voltammograms of polymer **12a** in film state coated on Pt electrodes in CH_3CN solution of 0.1 M Bu_4NBF_4 at a scan rate of 20 mV/s.

Table 2. Figure 6 depicted the UV and fluorescence spectra of polymer films **12c**, **13**, and **14** on ITO-glass.

Electrochemical Properties of Polymers. The electrochemical properties of these conjugated polymers were investigated using cyclic voltammetry. The polymer films dip-coated on a Pt electrode were scanned positively and negatively separately in a 0.1 M tetrabutylammonium tetrafloroborate (Bu_4NBF_4) solution in anhydrous acetonitrile. Figure 7 depicts the CV curves of both the p- and n-doping processes of polymer **12a** on a representative example. During the cathodic scan, the film of **12a** exhibited good reversible n-doping and dedoping processes. A reduction peak appeared at −1.85 V (E_{pc}) with the corresponding reoxidation peak at −1.81 V (E_{pa}). The onset potential of the reduction was −1.70 V. The electrochemical reduction process was very stable during repeat scanning with no obvious changes in the features of the CV. The n-doping of polymers was accompanied by an obvious color change (electrochromism) from red in the original films to green in the n-doped polymer films.

Other polymers depicted similar n-doping processes, except that the potential value shifted slightly with different alkyl pendant or backbones. Polymer **14** containing a 3,5-pyridinyl unit showed the highest reduction potential among those. However, it is noted that due to the presence of the electron-withdrawing pyridinyl unit, the reduction of all polymers is more facile than that electron-donating PBTBC$_x$ (E_{pc} = −2.14 to −2.39 V vs SCE)[20] and can be comparable to some good electron-transporting materials such as 2-(4-biphenylyl)-5-(4-*tert*-butylphenyl)-1,3,4-oxadiazole (PBD, E_{pc} = −1.97 V vs SCE) and copolymers containing PBD moieties.[37] This implies that the polymers may have electron-transporting properties similar to these typical electron-transporting materials.

From the cyclic voltamogram and UV−vis absorption spectra, the electron affinity (EA) of these polymers is ca. 2.57−2.60 eV, which is higher than previously reported green-emitting copolymers based on 3-alkylthienylene and phenylene units.[20,38] This may be attributed to the presence of electron-withdrawing pyridinyl moieties in the polymer backbone which decreases the LUMO energy. Consequently, these polymers may provide for more facile electron injections when used as active materials in PLEDs. In addition, facile electron injection from the cathode will make possible the use of more stable metals as the cathode.

The p-doping of **12a** depicted an oxidation peak at 1.01 V (E_{pa}) and a reduction peak at ca. 0.89 V, which is lower than that of poly[(2,5-bis(2′-thienyl)pyridine)] (P25H) (1.1 V vs SSCE)[39] prepared from electrochemical polymerization. The onset for p-doping is determined to be 0.86 V. During the oxidation process, the film changed from orange to brown color, with the polymer film being stable after multiple scans. Polymer **12b**, **12c**, and **13** showed a similar p-doping process. From the difference of onset potential between the reduction and oxidation processes, the band gaps of the polymers could be estimated, which were slightly larger than those evaluated from the absorption edge in the UV−vis spectra, as listed in Table 3.

XPS. The electronic environments of neutral and doped polymers were evaluated from the XPS core level spectra. The results suggest that both the sulfur and nitrogen atoms are oxidized in the polymer backbone.

Figure 8 shows the N(1s) signals for neutral and doped polymer **12a**, which is a representative example. The deconvolution of the N(1s) envelope of **12a** revealed only one component at 398.5 eV (fwhm = 1.60 eV). After doping, two nonequivalent nitrogen environments were revealed in the N(1s) spectra, as shown in Figure 8b. The low binding energy component at about 398.5 eV (fwhm = 1.60 eV) is attributable to neutral nitrogen. The high BE component (400.9 eV, fwhm = 1.60 eV), which has a chemical shift of about +2.4 eV from the neutral nitrogen, is associated with the oxidized pyridinium nitrogen.[40,41]

The deconvolution of the S(2p) envelope for neutral polymer **12a**, as shown in Figure 9a, revealed only one sulfur environment as a set of doublet [S($2p_{3/2}$) and S($2p_{1/2}$)] with spin−orbit splitting of 1.2 eV and area rations of 2:1. The binding energy of the S($2p_{3/2}$) peak is at ca. 163.8 eV (fwhm = 1.5 eV). These are attributable to neutral sulfur in the thienylene ring.[42] For doped samples, two sets of doublets were deconvoluted from the S(2p) curve with S($2p_{3/2}$) components located at 163.8 eV (fwhm = 1.5 eV) and 164.8 eV (fwhm = 1.5 eV), respectively (Figure 9b). The former originates similarly from neutral sulfur in the neutral polymer, while the latter suggests that some sulfur atoms are positively polarized or partially charged, a result of the oxidation of polymer chain by dopants.[42]

Conclusion

A novel series of donor−acceptor conjugated polymers comprising alternating bis(3-alkylthienylene) and para- or meta-linked pyridinyl repeating units were synthe-

Table 3. Summary of Onset and Peak Potentials of p- and n-Doping Processes and the Bandgap Values

	p-doping			n-doping			band gap
polymer	E_{on} (V)	E_{pa} (V)	E_{pc} (V)	E_{on} (V)	E_{pc} (V)	E_{pa} (V)	E_g[a] (eV)
12a	0.80	1.01	0.89	−1.65	−1.86	−1.82	2.45
12b	0.75	1.05	0.96	−1.68	−1.88	−1.82	2.43
12c	0.71	1.06	1.02	−1.70	−1.93	−1.84	2.41
13	0.90	1.03	0.94	−1.68	−1.90	−1.85	2.58
14	0.90	*b*	*b*	−1.75	−1.97	−1.88	2.65

[a] Electrochemical band gap. [b] Unresolved.

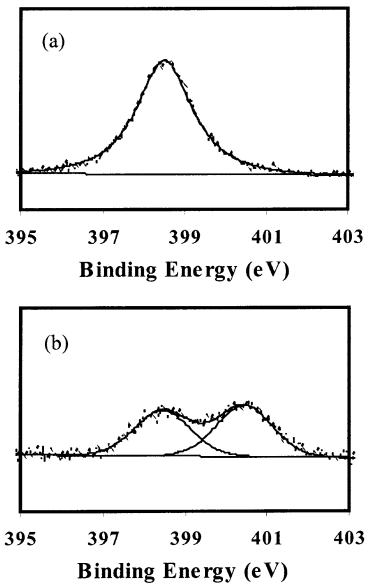

Figure 8. XPS spectra of polymer **12a**: (a) N(1s) spectrum of neutral polymer; (b) N(1s) spectrum of $FeCl_3$-doped polymer.

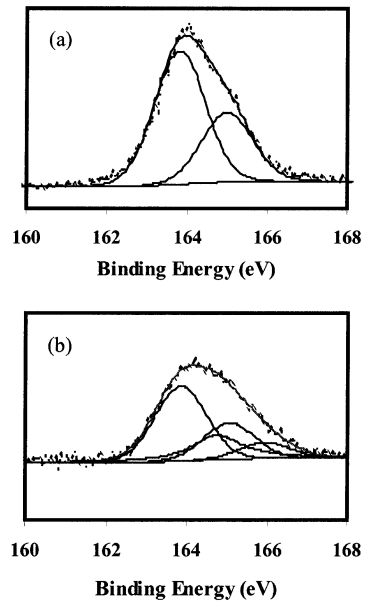

Figure 9. XPS spectra of polymer **12a**: (a) S(2p) spectrum of neutral polymer; (b) S(2p) spectrum of $FeCl_3$-doped polymer.

sized by a Stille coupling approach. The derived polymers depicted good solubility in common organic solvents such as chloroform, tetrahydrofuran, and trifloroacetic acid. Our investigations showed that the polymer electronic and optical properties were consistent with their conjugated backbone structure. They showed strong green fluorescence in their solution and film states with high photoluminescence quantum yields in solution. Polymers with meta-linkages exhibited blue shifts from those with para-linkages in their UV and fluorescence spectra. The optical behavior of these polymers in CF_3COOH solution depicted bathochromic shifts from those in $CHCl_3$ solution and interestingly showed nearly identical emission maxima although they have different backbone linkage structures. The derived polymers were electrically conductive when doped with I_2 and $FeCl_3$. FTIR and XPS investigations showed that doping-induced charge-transfer complexes were formed in polymers. The electrochemical behavior of the polymers depicted facile p- and n-doping characteristics and good electron-transporting properties ascribable to the introduction of electron-withdrawing pyridinyl unit. On the basis of these results, the novel polymers might be promising materials for applications in light-emitting diodes, rechargeable batteries, and light-emitting electrochemical cells.

References and Notes

(1) Broms, P.; Fahlman, M.; Xing, K. Z.; Salaneck, W. R.; Dannetun, P.; Cornil, J.; Dossantos, D. A.; Bredas, J. L.; Moratti, S. C.; Holmes, A. B.; Friend, R. H. *Synth. Met.* **1994**, *67*, 93−96.
(2) Fahlman, M.; Broms, P.; Dossantos, D. A.; Moratti, S. C.; Johansson, N.; Xing, K.; Friend, R. H.; Holmes, A. B.; Bredas, J. L.; Salaneck, W. R. *J. Chem. Phys.* **1995**, *102*, 8167−8174.
(3) Harrison, N. T.; Baigent, D. R.; Halls, J. J. M.; Pichler, K.; Friend, R. H. *Synth. Met.* **1996**, *76*, 43−45.
(4) Samuel, I. D. W.; Rumbles, G.; Collison, C. J.; Crystall, B.; Moratti, S. C.; Holmes, A. B. *Synth. Met.* **1996**, *76*, 15−18.
(5) Greenham, N. C.; Friend, R. H.; Bradley, D. D. C. *Adv. Mater.* **1994**, *6*, 491−494.
(6) Liu, Y. Q.; Li, Q. L.; Xu, Y.; Jiang, X. Z.; Zhu, D. B. *Synth. Met.* **1997**, *85*, 1279−1280.
(7) Rasmusson, J. R.; Broms, P.; Birgerson, J.; Erlandsson, R.; Salaneck, W. R. *Synth. Met.* **1996**, *79*, 75−84.
(8) Halls, J. J. M.; Walsh, C. A.; Greenham, N. C.; Marseglia, E. A.; Friend, R. H.; Moratti, S. C.; Holmes, A. B. *Nature (London)* **1995**, *376*, 498−500.
(9) Demanze, F.; Yassar, A.; Garnier, F. *Macromolecules* **1996**, *29*, 4267−4273.
(10) Roncali, J. *Chem. Rev.* **1997**, *97*, 173−205.
(11) Demanze, F.; Yassar, A.; Garnier, F. *Adv. Mater.* **1995**, *7*, 907.
(12) Lee, B. L.; Yamamoto, T. *Macromolecules* **1999**, *32*, 1375−1382.
(13) Saito, H.; Ukai, S.; Iwatsuki, S.; Itoh, T.; Kubo, M. *Macromolecules* **1995**, *28*, 8363−8367.
(14) Zhang, Q. T.; Tour, J. M. *J. Am. Chem. Soc.* **1998**, *120*, 5355−5362.
(15) Naka, K.; Umeyama, T.; Chujo, Y. *Macromolecules* **2000**, *33*, 7467−7470.
(16) Karikomi, M.; Kitamura, C.; Tanaka, S.; Yamashita, Y. *J. Am. Chem. Soc.* **1995**, *117*, 6791−6792.
(17) Yamamoto, T.; Takagi, M.; Kizu, K.; Maruyama, T.; Kubota, K.; Kanbara, H.; Kurihara, T.; Kaino, T. *J. Chem. Soc., Chem. Commun.* **1993**, 797−798.
(18) Yamamoto, T.; Zhou, Z. H.; Kanbara, T.; Shimura, M.; Kizu, K.; Maruyama, T.; Nakamura, Y.; Fukuda, T.; Lee, B. L.; Ooba, N.; Tomaru, S.; Kurihara, T.; Kaino, T.; Kubota, K.; Sasaki, S. *J. Am. Chem. Soc.* **1996**, *118*, 10389−10399.
(19) Ng, S. C.; Xu, J. M.; Chan, H. S. O. *Synth. Met.* **1998**, *92*, 33−37.

(20) Ng, S. C.; Xu, J. M.; Chan, H. S. O. *Macromolecules* **2000**, *33*, 7349−7358.
(21) Irvin, D. J.; DuBois, C. J.; Reynolds, J. R. *Chem. Commun.* **1999**, 2121−2122.
(22) Jenkins, I. H.; Salzner, U.; Pickup, P. G. *Chem. Mater.* **1996**, *8*, 2444−2450.
(23) Kaeriyama K.; Sato, M.; Tanaka, S. *Synth. Met.* **1987**, *18*, 233.
(24) Ng, S. C.; Lu, H. F.; Chan, H. S. O.; Fujii, A.; Laga, T.; Yoshino, K. *Adv. Mater.* **2000**, *12*, 1122.
(25) Ng, S. C.; Lu, H. F.; Chan, H. S. O.; Fujii, A.; Laga, T.; Yoshino, K. *Macromolecules* **2001**, *34*, 6895−6903.
(26) Wang, H.; Helgeson, R.; Ma, B.; Wudl, F. *J. Org. Chem.* **2000**, *65*, 5862−5867.
(27) Ruiz, J. P.; Dharia, J. R.; Reynolds, J. R.; Buckley, L. J. *Macromolecules* **1992**, *25*, 849−860.
(28) McCullough, R. D.; Lowe, R. D.; Jayaraman, M.; Anderson, D. L. *J. Org. Chem.* **1993**, *58*, 904−912.
(29) Li, J.; Pang, Y. *Macromolecules* **1997**, *30*, 7487−7492.
(30) Sato M.; Tanaka S.; Kaeriyama, K. *Makromol. Chem.* **1987**, *188*, 1763.
(31) Inganas, O.; Salaneck, W. R.; Osterholm, J. E.; Laakso, J. *Synth. Met.* **1988**, *22*, 395−406.
(32) Fu, D. K.; Xu, B.; Swager, T. M. *Tetrahedron* **1997**, *53*, 15487−15494.
(33) Yamamoto, T.; Sugiyama, K.; Kushida, T.; Inoue, T.; Kanbara, T. *J. Am. Chem. Soc.* **1996**, *118*, 3930−3937.
(34) Johnson, E. G.; Willardson, R.; Beer, A. C. *Semiconductors and Semimetals*; Academic Press: New York, 1967; p 153.
(35) Roux, C.; Bergeron, J. Y.; Leclerc, M. *Makromol. Chem.* **1993**, *194*, 869−877.
(36) Roux, C.; Leclerc, M. *Chem. Mater.* **1994**, *6*, 620−624.
(37) Janietz, S.; Wedel, A. *Adv. Mater.* **1997**, *9*, 403.
(38) Ng, S. C.; Xu, J. M.; Chan, H. S. O.; Fujii, A.; Yoshino, K. *J. Mater. Chem.* **1999**, *9*, 381−385.
(39) Tanaka, S.; Sato, M. A.; Kaeriyama, K. *J. Macromol. Sci., Chem.* **1987**, *A24*, 749.
(40) Ng, K. T.; Hercules, D. M. *J. Am. Chem. Soc.* **1975**, *97*, 4169.
(41) Tan, K. L.; Tan, B. T. G.; Kang, E. T.; Neoh, K. G. *J. Mol. Electron.* **1990**, *6*, 5−13.
(42) Kang, E. T.; Neoh, K. G.; Tan, K. L. *Phys. Rev. B* **1991**, *44*, 10461−10469.

MA021082+